J Mol Med (2017) 95:601–613
DOI 10.1007/s00109-017-1538-0

JMolMed

ORIGINAL ARTICLE

DNA hypermethylation of *sFRP5* contributes to indoxyl sulfate-induced renal fibrosis

Yanlin Yu[1] · Xu Guan[1] · Ling Nie[1] · Yong Liu[1] · Ting He[1] · Jiachuan Xiong[1] · Xinli Xu[1] · Yan Li[1] · Ke Yang[1] · Yiqin Wang[1] · Yunjian Huang[1] · Bing Feng[1] · Jingbo Zhang[1] · Jinghong Zhao[1]

Received: 6 November 2016 / Revised: 24 March 2017 / Accepted: 27 April 2017 / Published online: 15 May 2017

Abstract
Renal fibrosis is the most common outcome of chronic kidney disease (CKD), while the pathogenesis of renal fibrosis is not fully understood. In this study, we first showed that the progress of renal fibrosis was positively related to serum levels of indoxyl sulfate, a typical protein-bound toxin, and that there was a close correlation between serum indoxyl sulfate levels and β-catenin expression in the kidneys ($r = 0.908, p < 0.001$) of CKD patients. We then demonstrated that intraperitoneal injections of indoxyl sulfate (100 mg/kg/day) for 4 weeks in uninephrectomized mice explicitly induced renal fibrosis, which was accompanied by a significant activation of Wnt/β-catenin signaling. In vitro investigations in human renal tubular HK-2 cells revealed that indoxyl sulfate exhibited a potent ability to induce Wnt/β-catenin activation through the downregulation of *sFRP5*, a gene that codes for an extracellular antagonist of Wnt signaling, by increasing the DNA methylation level of its promoter CpG islands. The increased expression of DNA methyltransferases following the activation of ROS/ERK1/2 signaling was responsible for the DNA hypermethylation of *sFRP5* induced by indoxyl sulfate. Conversely, treatment with 5-aza-2′-deoxycytidine, an inhibitor of DNA methyltransferases, significantly reduced indoxyl sulfate-induced *sFRP5* downregulation and Wnt/β-catenin activation. In vivo, intraperitoneal injections of recombinant *sFRP5* protein or 5-aza-2′-deoxycytidine substantially alleviated renal fibrosis in indoxyl sulfate-treated uninephrectomized mice. Our results suggest that indoxyl sulfate promotes renal fibrosis through the induction of DNA hypermethylation of *sFRP5*, and thereafter the activation of Wnt/β-catenin signaling. These findings provide new insights into the pathogenesis of renal fibrosis in CKD patients.

Key messages
- IS induces renal fibrosis by increasing ß-catenin expression in CKD mice.
- IS-induced Wnt signaling activation is due to *sFRP5* hypermethylation in HK-2 cells.
- ROS/ERK1/2 signaling activation is involved in IS-induced *sFRP5* hypermethylation.
- *sFRP5* upregulation attenuates IS-induced renal fibrosis by inhibiting Wnt signaling.

Keywords Indoxyl sulfate · Renal fibrosis · DNA methylation · *sFRP5* · Wnt/β-catenin

Introduction

Nowadays, the prevalence of CKD is a global challenge. Renal fibrosis, which is characterized by the abnormal accumulation of extracellular matrix in the renal interstitium, is the most common outcome of CKD [1–3]. Previous studies have shown that traditional risk factors, including immunological dysfunction, renin-angiotensin-aldosterone system activation, dyslipidemia, and hyperglycemia play important roles in the development of renal fibrosis in CKD patients [4–7], whereas the influence of the uremic milieu on the progression of renal fibrosis has not

Yanlin Yu and Xu Guan contributed equally to this work.

Electronic supplementary material The online version of this article (doi:10.1007/s00109-017-1538-0) contains supplementary material, which is available to authorized users.

✉ Jinghong Zhao
zhaojh@tmmu.edu.cn

[1] Department of Nephrology, Institute of Nephrology of Chongqing and Kidney Center of PLA, Xinqiao Hospital, Third Military Medical University, Chongqing 400037, People's Republic of China

been well demonstrated. It has been shown that the uremic toxins accumulated in the blood of patients with CKD [8], and the renal fibrosis progresses rapidly during this period. In recent years, many studies have reported the deleterious effects of uremic toxins, especially protein-bound toxins such as indoxyl sulfate (IS) and p-cresol (PCS), on the functions of the kidneys and the cardiovascular system in patients with CKD [9–12]. Interestingly, in addition to inhibiting the proliferation of tubular cells, protein-bound toxins have also been demonstrated to increase collagen deposition in the renal tubule interstitium in uninephrectomized mice [13–15], suggesting that uremic toxins may contribute to the development of renal fibrosis in patients with CKD. However, the in-depth molecular mechanisms underlying the role of uremic toxins in promoting renal fibrosis are largely unknown.

Accumulating evidence indicates that the Wnt/β-catenin signaling pathway plays a key role in the process of renal fibrosis and that renal fibrosis can be significantly ameliorated by Wnt antagonists [16, 17], but whether Wnt/β-catenin signaling is involved in IS-induced renal fibrosis has never been revealed. As previously reported, the secreted frizzled-related proteins (sFRPs) function as Wnt antagonists by binding and inactivating Wnt ligands, and inhibition of sFRPs leads to Wnt/β-catenin activation [18]. The aberrant DNA methylation of sFRPs has been demonstrated to be involved in the activation of Wnt/β-catenin signaling, promoting the progress of various cancers [19, 20]. Previously reported, epigenetic DNA methylation, which is usually triggered by inflammation and oxidative stress in uremic milieus has attracted attention [21, 22]. Moreover, protein-bound toxins with the capacity to initiate oxidative stress have been reported to induce DNA hypermethylation of target genes [23]. Therefore, it is necessary to investigate the effects of protein-bound toxins on the DNA methylation of sFRP genes and the role of these effects in the progression of renal fibrosis.

In this study, we analyzed the relationship between IS and the activation of Wnt/β-catenin signaling to deeply explore the pathogenesis of CKD-associated renal fibrosis. Our results revealed the critical role of *sFRP5* DNA hypermethylation in IS-induced renal fibrosis.

Results

Positive correlation between serum IS levels and renal fibrosis in CKD patients

Thirty-four patients with estimated glomerular filtration rates (eGFRs) of 6.92–148.42 ml/min/1.73 m^2 were enrolled in this study. The eGFRs, serum IS levels, and degree of renal fibrosis in the kidneys were detected separately. Serum IS levels and fibrotic area with Masson's trichrome staining both gradually increased with the decline of eGFR (Fig. 1a, b). It was found that the progression of renal fibrosis was positively related to increases in serum IS (Fig. 1c). These data suggest that a correlative relationship may exist between IS and the progression of renal fibrosis in CKD patients.

IS injection-induced renal fibrosis is accompanied by increased expression of β-catenin in the kidneys of CKD mice

To confirm the relationship between IS and the activation of Wnt/β-catenin signaling in the kidneys during the progression of renal fibrosis, we treated uninephrectomized CD-1 mice with IS (100 mg/kg per day) via intraperitoneal injections for 4 weeks and found that IS injection induced a 5-fold increase in the serum level of IS (Fig. 2a). Meanwhile, significant increases in β-catenin, active-β-catenin, and α-SMA expression levels and collagen deposition were observed in the remaining kidney in IS-treated CKD mice (Fig. 2b–d). We also found that IS inhibited the expression of klotho, which is an endogenous antagonist of Wnt/β-catenin signaling. In addition, we further explored the expression of klotho in IS-treated HK-2 cells. The decreased expression of klotho was observed in IS-treated HK-2 cells, as revealed by western blot (Fig. 2e). We then detected the direct effect of IS on the expression of β-catenin in cultured HK-2 cells and found that β-catenin expression was upregulated at translational levels by IS in a dose-dependent manner (Fig. 2f). These data suggest that the activation of Wnt/β-catenin signaling may be implicated in IS-induced renal fibrosis.

IS reduces the expression of the Wnt antagonistic gene *sFRP5* in renal tubular cells

To investigate the mechanisms underlying the effect of IS on Wnt/β-catenin activation in renal tubular cells, we measured the mRNA expressions of *sFRP* genes, which negatively regulate the activation of Wnt/β-catenin signaling, in IS-treated HK-2 cells by semi-quantitative PCR. The results indicated that the expression of *sFRP1–3* was very weak in HK-2 cells, while the expression of *sFRP4* and *sFRP5* was strong. Notably, IS suppressed *sFRP5* mRNA expression but not sFRP4 in HK-2 cells in a dose-dependent manner (Fig. 3a). Concordantly, a dose-dependent reduction in *sFRP5* protein but not sFRP4 expression was also observed in HK-2 cells after IS treatment (Fig. 3b). Next, we detected *sFRP5* expression in tubular cells in renal biopsy samples from patients with CKD by immunohistochemical staining. As shown in Fig. 3c, *sFRP5* expression was significantly decreased in renal tubular cells from CKD patients with renal fibrosis compared with normal control cells. In addition, a significant reduction in the expression of *sFRP5* both at the mRNA and protein level was found in IS-injected CKD mice (Fig. 3d–f). These results indicate that IS has the ability to silence *sFRP5* gene

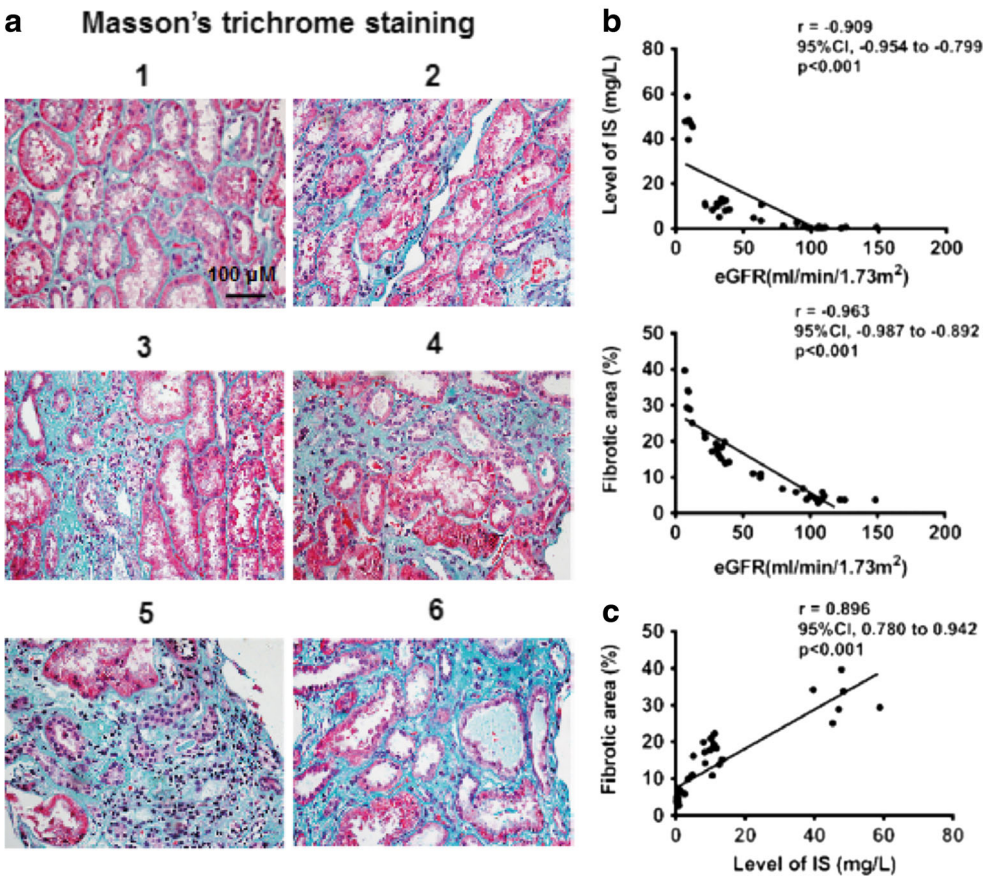

Fig. 1 Serum levels of IS are associated with renal fibrosis in CKD patients. **a** Representative Masson's trichrome staining in six CKD patients (the eGFRs of six patients were as follows: (1) 99.9 ml/min/1.73 m^2, (2) 97.4 ml/min/1.73 m^2, (3) 63.1 ml/min/1.73 mh6, (4) 57.6 ml/min/1.73 m^2, (5) 9.8 ml/min/1.73 m^2, and (6) 10.8 ml/min/1.73 m^2). **b**, **c** The correlation between eGFR, the serum IS level, and fibrotic area (%). Statistical differences were determined based on Spearman's correlation coefficient

expression, which may lead to the activation of Wnt/β-catenin signaling that contributes to the development of renal fibrosis.

IS downregulates *sFRP5* gene expression via DNA hypermethylation

Because the gene expression of sFRP is usually regulated by DNA methylation and IS has the potential to induce DNA methylation [23], we then measured the effect of IS on *sFRP5* DNA methylation. As shown in Fig. 4a, the DNA methylation level of *sFRP5* was markedly elevated in HK-2 cells after treatment with IS at concentrations of 10 and 50 mg/L. In addition, the mRNA expressions of DNA methyltransferases (DNMTs), including DNMT1, DNMT3a, and DNMT3b were significantly upregulated in IS-treated HK-2 cells (Fig. 4b). Moreover, an evident increase in the protein expression of DNMT1, 3a, 3b was also observed after IS treatment (Fig. 4c).

Subsequently, CpG island prediction software analysis found that the typical CpG islands in the transcription start region of the *sFRP5* gene (Fig. 4d). Bisulfite-sequencing PCR (BSP) was performed to further confirm the MSP results. Amplified fragments were cloned and sequenced for each amplification product from individual group. As shown in Fig. 4e, the detected CpG islands located in the promoter region of *sFRP5* contains 24 CpG dinucleotides. The frequency of methylated CpG dinucleotides in this region in IS-treated HK-2 cells was 40.3 ± 7.3%, which was much higher than that in the control group (6.2 ± 5.7%), further confirming that IS can induce *sFRP5* DNA hypermethylation in HK-2 cells.

sFRP5 DNA hypermethylation contributes to the activation of Wnt/β-catenin signaling in IS-treated HK-2 cells

To confirm whether *sFRP5* DNA hypermethylation is involved in the IS-induced activation of Wnt/β-catenin signaling, HK-2 cells were pretreated with the DNMTs inhibitor 5Aza-2dc before incubation with IS (50 mg/L). We first found that the IS-induced increase of DNMT1 expression and *sFRP5* gene hypermethylation in HK-2 cells were significantly inhibited by 5Aza-2dc in a dose-dependent manner (Fig. 5a, b). Then, we found that the IS-induced downregulation of *sFRP5* and upregulation of β-catenin were also markedly suppressed by 5Aza-2dc (Fig. 5c, d). Furthermore, an immunoprecipitation assay revealed that incubation with IS significantly reduced the binding of *sFRP5* to Wnt5a in HK-2 cells and that this inhibitory effect of IS could be reversed by 5Aza-2dc (Fig. 5e). Therefore, IS-induced *sFRP5* DNA

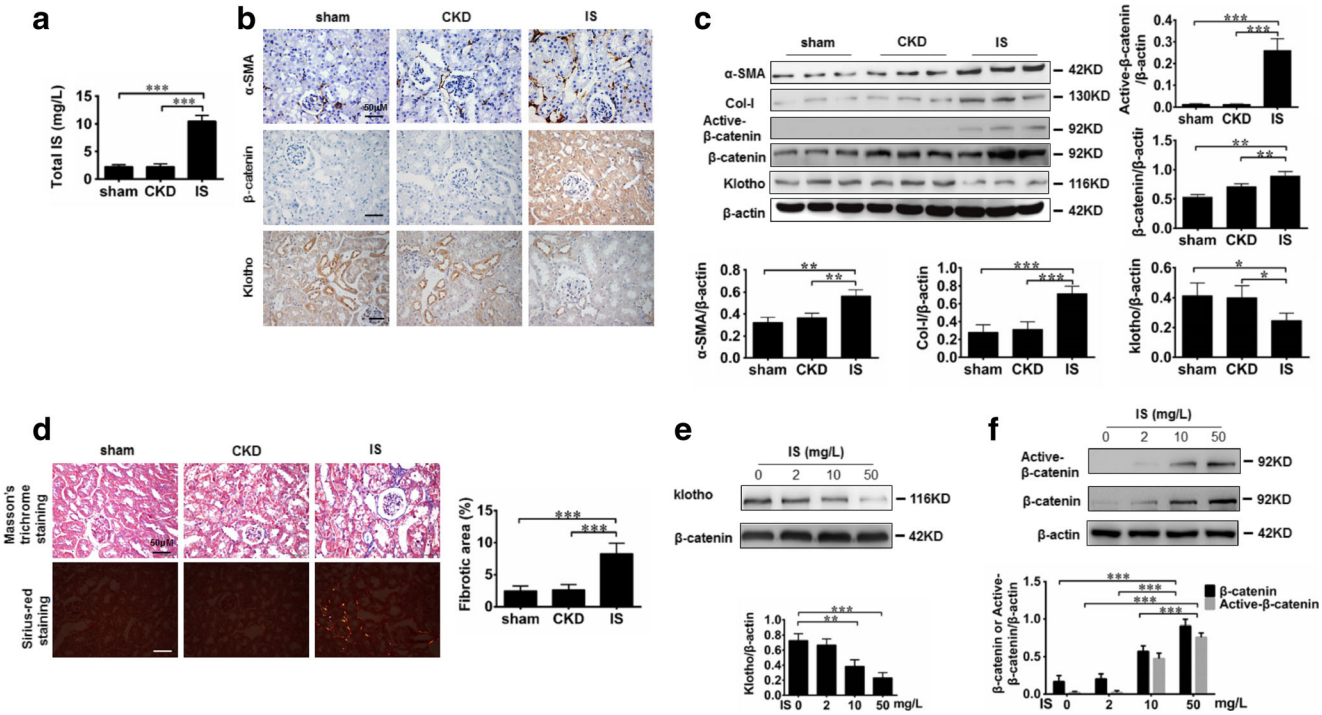

Fig. 2 IS induces renal fibrosis and activates the Wnt/β-catenin signaling pathway. **a** The serum IS levels in IS-injected uninephrectomized mice were higher than those of control mice and non-IS-injected uninephrectomized mice. **b, c** The expression of α-SMA, collagenase I, β-catenin, and klotho in the kidneys was significantly increased in uninephrectomized mice after IS injection, as assessed by western blotting, α-SMA, β-catenin, and klotho also detected by immunohistochemical staining. **d** Significantly increased collagen deposition was observed in the kidneys of IS-injected CKD mice (Masson's trichrome staining, Sirius red staining). Under polarized light, the larger collagen fibers (type I) are bright yellow or orange. The fibrotic area (*blue area*) was quantified ($n = 8$ mice). **e** In HK-2 cells, the protein expression of β-catenin and active-β-catenin was increased in a dose-dependent manner after treatment with IS (2, 10, and 50 mg/L) for 72 h. Data are the means ± SEM. $^{**}P < 0.01$; $^{***}P < 0.001$ (color figure online)

hypermethylation possibly contributes to the activation of Wnt/β-catenin signaling in renal tubular cells.

ROS/ERK1/2 signaling activation is involved in IS-induced *sFRP5* hypermethylation

We next investigated the role of oxidative stress and its downstream signaling in IS-induced *sFRP5* DNA hypermethylation as previous studies have shown that oxidative stress is an important risk factor for DNA hypermethylation and IS can induce oxidative stress. As shown in Fig. 6a, b, IS significantly promoted ROS production in HK-2 cells in a dose- and time-dependent manner, and this increase was accompanied by an increase in the phosphorylation of p44/42 MAPK (ERK1/2). By contrast, pretreatment with NAC (a ROS scavenger) and the ERK1/2 inhibitor U0126 markedly suppressed the phosphorylation of ERK1/2 and the DNA hypermethylation of *sFRP5* (Fig. 6c, d). Meanwhile, the IS-induced increase in DNMT1 expression and downregulation of *sFRP5* were also significantly inhibited by NAC and U0126 pretreatments (Fig. 6e). These results suggest that ROS/ERK1/2 signaling activation is involved in IS-induced *sFRP5* hypermethylation.

Blocking DNA methylation and supplementation with recombinant *sFRP5* protein both ameliorate renal fibrosis by inhibiting Wnt/β-catenin activation in IS-injected CKD mice

In uninephrectomized mice, intraperitoneal injections of IS (100 mg/kg/day for 4 weeks) significantly increased the DNA methylation status of the *sFRP5* gene in the remaining kidney, whereas treatment with 5Aza-2dc (0.35 mg/kg/48 h, intraperitoneal injection) substantially decreased the DNA methylation of *sFRP5* induced by IS, as assayed by MSP (Fig. 7a, b). Moreover, western blotting showed that treatment with 5Aza-2dc appeared to reverse the reduction in *sFRP5* expression in the kidneys of IS-injected mice (Fig. 7c), demonstrating that the capacity for IS to downregulate *sFRP5* expression is mainly due to its ability to induce DNA hypermethylation.

Finally, we evaluated the treatment effects of 5Aza-2dc and recombinant *sFRP5* protein (0.01 or 0.02 mg/kg/48 h) on renal fibrosis in IS-injected CKD mice. As shown in Fig. 8a, b, both the 5Aza-2dc and *sFRP5* treatments significantly ameliorated renal fibrosis in IS-injected mice, as assessed by Masson's trichrome staining, Sirius red staining, and α-SMA-positive staining. Notably, the expression of both β-

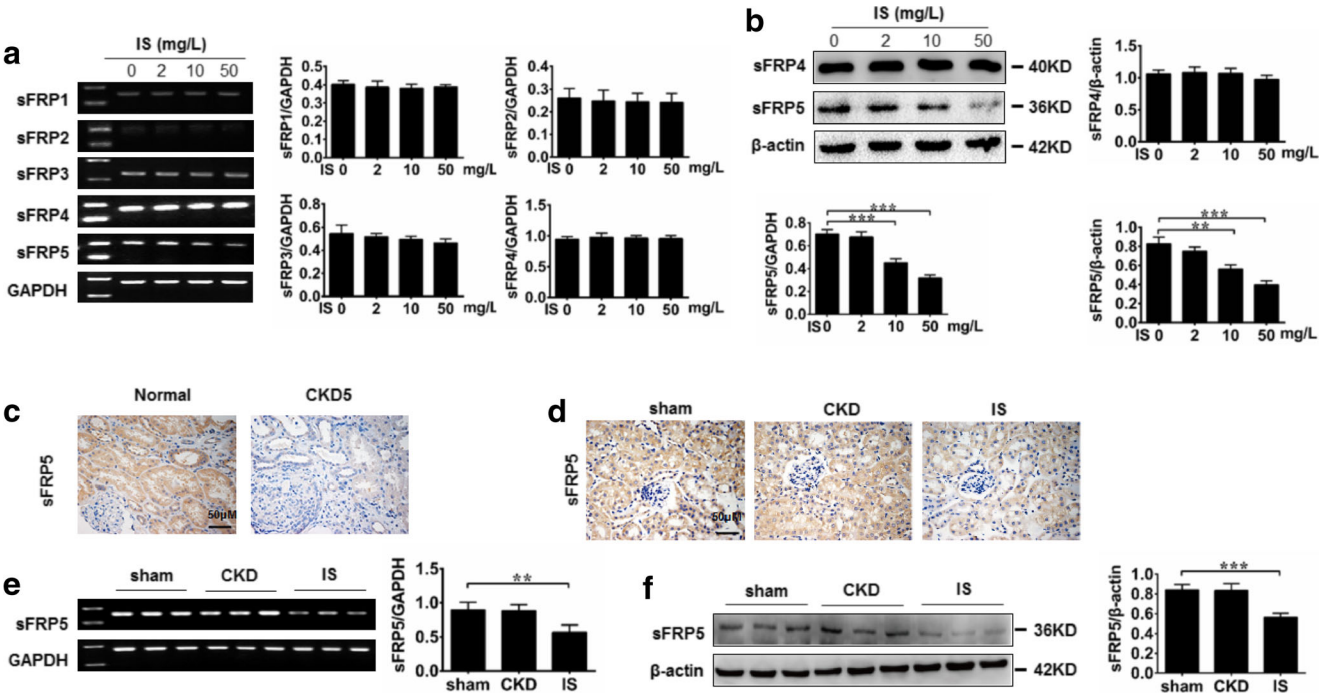

Fig. 3 IS suppresses *sFRP5* expression in HK-2 cells and individuals CKD. HK-2 cells were exposed to different concentrations of IS (2, 10, and 50 mg/L) for 72 h. **a** *sFRP1–5* mRNA expression was detected by RT-PCR, and a substantial decrease in *sFRP5* mRNA were observed in IS-treated HK-2 cells. **b** The decreased expression of the sFRP4 and *sFRP5* protein was also observed in IS-treated HK-2 cells at concentrations of 10 and 50 mg/L. **c** *sFRP5* expression was significantly decreased in kidney biopsy samples from patients with stage 5 CKD compared with the expression in the normal kidney samples. **d** *sFRP5* protein levels in the kidneys were reduced in IS-injected CKD mice (immunohistochemical staining). **e**, **f** A decrease in *sFRP5* mRNA and protein expression in the kidneys was observed in IS-injected CKD mice ($n = 8$ mice). Data are the means ± SEM. $^{**}P < 0.01$; $^{***}P < 0.001$

catenin and active-β-catenin in the kidney was also significantly reduced after the 5Aza-2dc and *sFRP5* treatments (Fig. 8a–d). These data demonstrate that exogenous supplementation with the *sFRP5* protein or the upregulation of *sFRP5* expression by blocking DNA hypermethylation can attenuate renal fibrosis via the suppression of Wnt/β-catenin activation. In addition, we examined the expression of klotho, which can be epigenetically regulated by IS. We found that both the 5Aza-2dc and *sFRP5* treatments significantly increased klotho expression in IS-injected mice when compared with the mice treated with IS alone (Fig. 8a).

Discussion

Tubulointerstitial fibrosis and uremic toxin accumulation are two hallmarks of chronic renal failure, and the relationship between these two pathological features in CKD needs to be clarified. In the present study, we not only addressed the role of protein-bound uremic toxin accumulation inducing renal fibrosis but also revealed that IS-induced *sFRP5* DNA hypermethylation is an important contributor to the activation of the Wnt/β-catenin signaling that plays a key role in renal fibrosis, thereby providing novel insight into the mechanisms underlying the effect of protein-bound uremic toxins on the progression of renal fibrosis in CKD patients. As the progression of renal fibrosis may aggravate renal dysfunction, which in turn promotes uremic toxin accumulation, our findings provide a deeper understanding of the progressive renal lesion in CKD patients.

IS, a typical protein-bound toxin that accumulates in the serum of CKD patients, is difficult to remove from the blood by conventional dialysis [24]. In recent years, the role of IS in the development of CKD and its associated pathological complications has attracted increasing attention due to its distinctive physicochemical properties and toxic effects. Here, we first show that the progression of renal fibrosis is positively related to serum IS levels in patients with CKD based on an analysis of clinical data. Furthermore, we confirmed that renal fibrosis can be induced in uninephrectomized mice via IS injections, which is consistent with previous reports [23, 25]. These findings provide new and compelling evidence that IS accumulation is an important risk factor for the development of renal fibrosis in CKD patients.

Wnt/β-catenin signaling is an important cellular signal transduction pathway and is involved in various physical and pathological processes [26]. It has been reported that the activation of Wnt/β-catenin signaling plays a key role in progressive interstitial fibrosis in a model of unilateral ureteral obstruction (UUO) [27, 28], and the inhibition of Wnt/β-

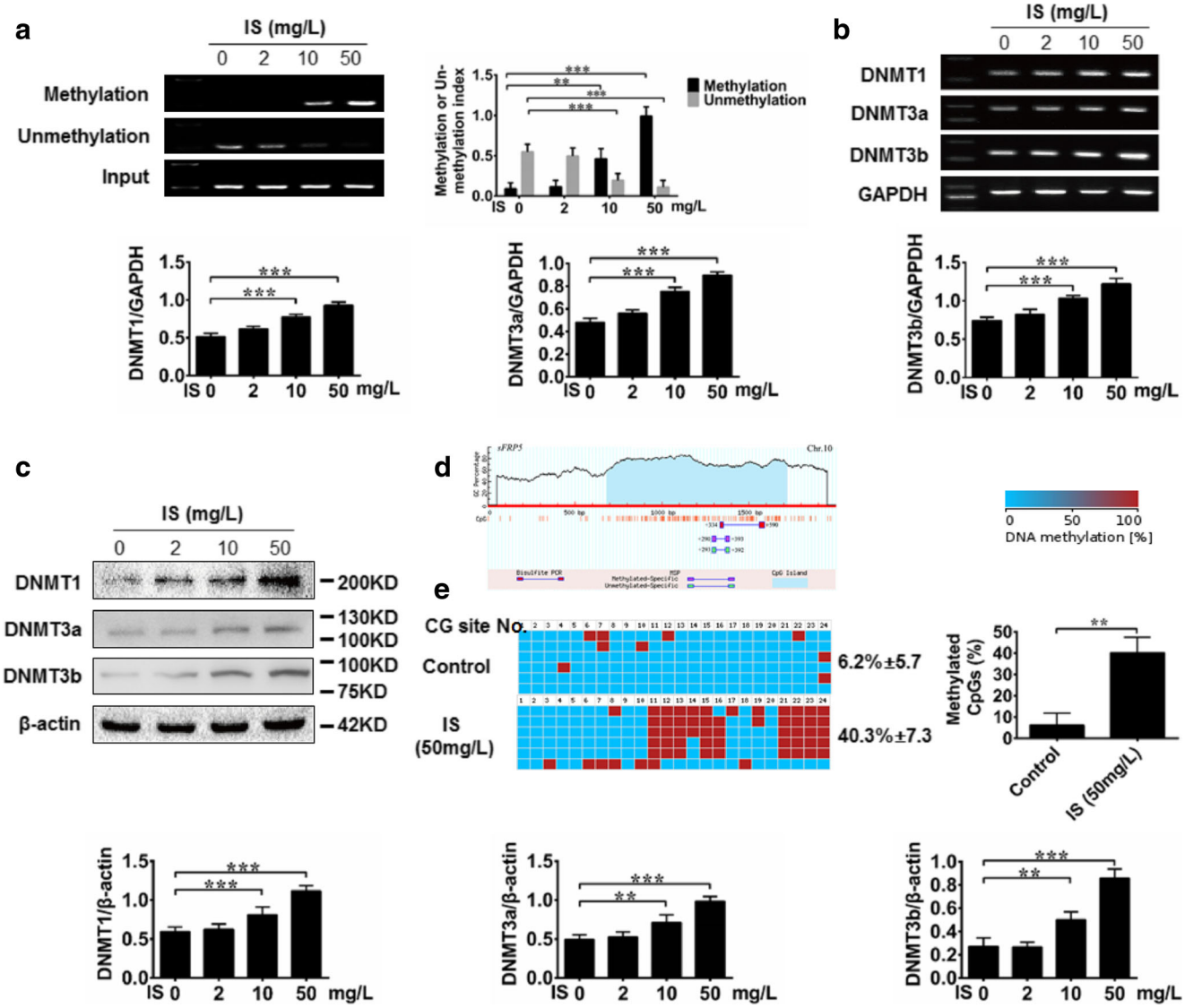

Fig. 4 IS induces *sFRP5* DNA hypermethylation in HK-2 cells. HK-2 cells were incubated with different concentrations of IS (2, 10, and 50 mg/L) for 72 h. **a** As revealed by a methylation-specific PCR (MSP) analysis, the DNA methylation level of the *sFRP5* gene was dramatically elevated in IS-treated HK-2 cells in a dose-dependent manner. **b** IS promoted DNMT1, 3a, and 3b mRNA expression in HK-2 cells at concentrations of 10 and 50 mg/L, as assessed by RT-PCR. **c** The protein level of DNMT1, 3a, 3b, measured by western blotting, was increased in HK-2 cells treated with IS at 10 and 50 mg/L. **d** Diagram of *sFRP5* promotor region. Analysis of CpG islands and primers for BSP or MSP were designed by MethPrimer software. **e** Quantitative DNA methylation analysis of the *sFRP5* gene promotor across multiple CpG sites (totally 24 sites), as assayed by BSP. *Blue*: unmethylation; *red*: methylation. Data are the means ± SEM. $^{**}P < 0.01$; $^{***}P < 0.001$ (color figure online)

catenin signaling is conducive to the attenuation of renal fibrosis [27, 29]. Mechanistic studies have revealed that the activation of Wnt/β-catenin signaling results in collagen deposition and renal fibrosis progression through the upregulation of MMP-7 expression, activation of the RAAS system and increases in the expression of Snail, along with other processes [27, 30, 31]. In our study, the results of both the in vivo and in vitro investigations demonstrate for the first time that Wnt/β-catenin signaling is involved in IS-induced renal fibrosis.

It is well known that sFRPs are extracellular Wnt antagonists that negatively regulate the activation of Wnt/β-catenin signaling by binding directly with Wnt ligands [32]. There are five members (sFRP1–5) of the sFRP family [18]. It has been reported that the downregulation of sFRPs contributes to the development of tumors via the activation of Wnt/β-catenin signaling [33–35]. The role of sFRPs in the inhibition of Wnt signaling in renal fibrosis is very interesting. In UUO mice, Wnt/β-catenin signaling has been shown to be activated after surgery, whereas intraperitoneal injections of recombinant sFRP4 protein significantly alleviate the progression of renal fibrosis via downregulation of β-catenin expression in tubular epithelial tissue [17]. Furthermore, *sFRP1* knockout mice show a significant increase in the expression of

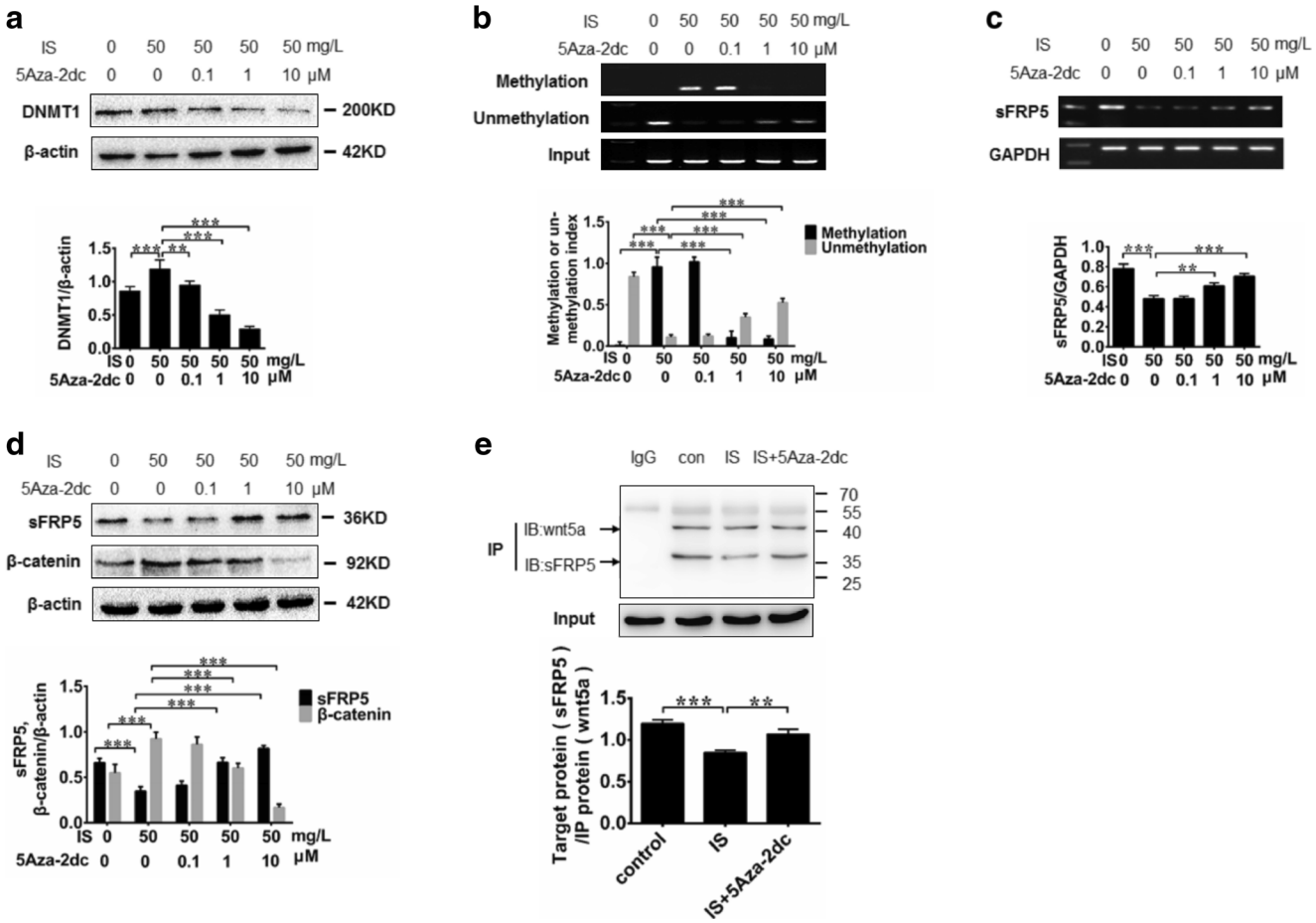

Fig. 5 A DNA methylation inhibitor attenuates the IS-induced *sFRP5* hypermethylation and the activation of Wnt/β-catenin signaling. HK-2 cells were cultured with 50 mg/L IS for 72 h after pretreatment with different concentrations of 5Aza-2dc (0.1, 1, and 10 μM) for 1 h. **a** The DNA methylation inhibitor 5Aza-2dc alleviated the IS-induced increase in DNMT1 expression in a dose-dependent manner. **b** 5Aza-2dc inhibited the IS-induced increase in *sFRP5* DNA hypermethylation in HK-2 cells. **c**, **d** 5Aza-2dc reversed the IS-induced decrease in *sFRP5* mRNA and protein expression and the increased protein expression of β-catenin in HK-2 cells. **e** 5Aza-2dc inhibited the IS-induced decrease in the ability of *sFRP5* to bind to Wnt5a in HK-2 cells, as assessed by immunoprecipitation analysis. Data are the means ± SEM. $^{**}P < 0.01$; $^{***}P < 0.001$

myofibroblast markers, followed by the activation of the non-canonical Wnt/PCP signaling pathway, in renal tubular epithelial cells after UUO [36]. These findings indicate that sFRPs are intrinsic inhibitors of renal fibrosis that act by restraining Wnt signaling. However, the effects of IS on the regulation of sFRPs and its role in IS-induced renal fibrosis are unclear. Here, we showed that sFRP4 and *sFRP5* were strongly expressed in human renal tubular HK-2 cells and that only *sFRP5* expression was significantly inhibited by IS. Moreover, *sFRP5* expression was significantly downregulated in renal tubular epithelial cells in uninephrectomized mice after intraperitoneal injection with IS, which was followed by the increased expression of β-catenin, suggesting that IS has the potential to activate Wnt/β-catenin signaling via the suppression of *sFRP5* expression. It is worth noting that our findings are different than those reported by Surendran et al., who showed that the expression of sFRP4 but not *sFRP5* decreased in the kidneys after UUO surgery [17]. We think that this discrepancy may be due to the different responses of these two genes to different stimuli.

As previously reported, DNA methylation is the predominant reason for the downregulation of sFRPs and the consequent activation of Wnt/β-catenin signaling. For instance, *sFRP1* silencing due to aberrant DNA hypermethylation activates the Wnt/β-catenin pathway and contributes to increases in cell growth and proliferation in hepatocellular carcinoma [37]. A previous study showed that *sFRP2* was methylated in 70% of prostate cancer specimens and that *sFRP5* was methylated in 60% of cells from two different prostate cancer cell lines, which might be the main reason for the aberrant activation of Wnts in prostate cancer cells [38]. Interestingly, IS has been confirmed to be capable of inducing the hypermethylation of the klotho gene, which is mainly expressed in renal tubular cells and plays a protective role in the kidneys [23]. In this study, we found that IS has the potential to increase the expression of DNMTs, and the decreased expression of

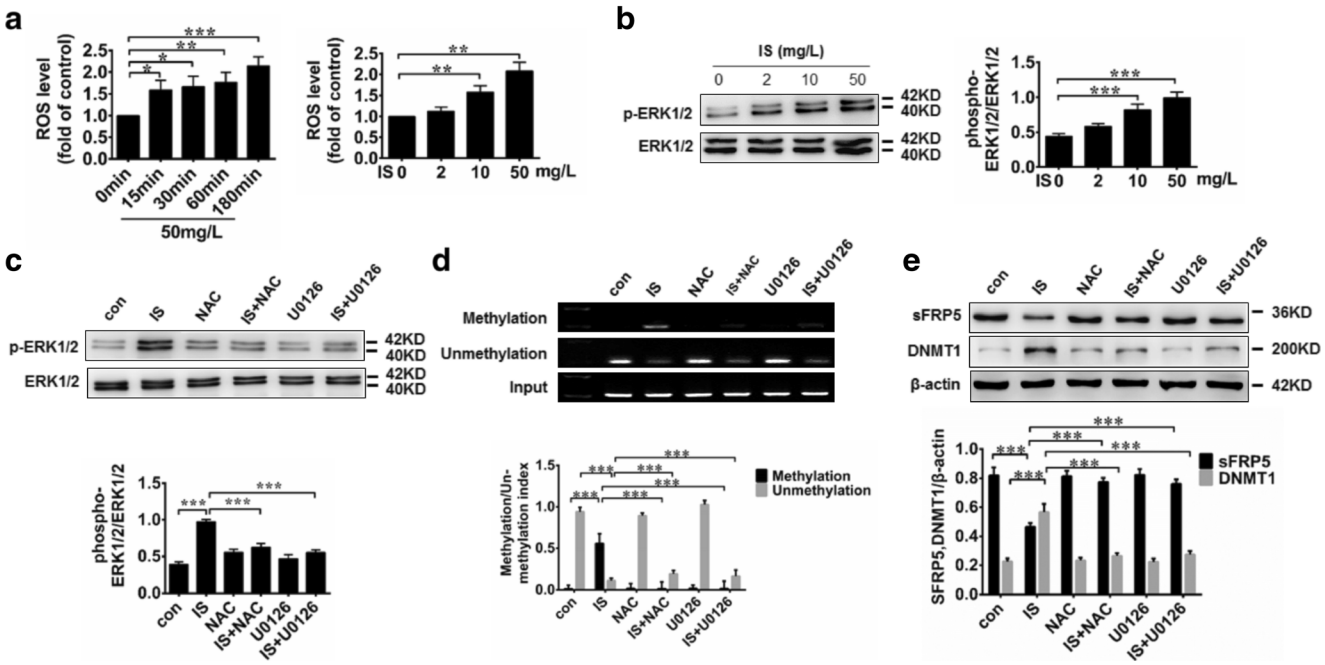

Fig. 6 IS induces *sFRP5* hypermethylation through the activation of ROS/ERK1/2 signaling. **a** DCF fluorescence analysis demonstrated that IS promotes ROS production in HK-2 cells in a dose- and time-dependent manner. HK-2 cells were treated with 50 mg/L IS for different times (15, 30, 60, and 180 min) or were treated with different concentrations of IS (2, 10, and 50 mg/L) for 3 h. **b** IS stimulated the phosphorylation of ERK1/2 in a dose-dependent manner. **c**–**e** Pretreatment of HK-2 cells with 5 mmol/L N-acetyl-L-cysteine (NAC) or 10 mmol/L U0126 for 1 h significantly attenuated the IS-induced phosphorylation of ERK1/2, DNA hypermethylation of *sFRP5* and increase in DNMT1 expression and decrease in *sFRP5* protein expression. Data are the means ± SEM. $^{*}P < 0.05$; $^{**}P < 0.01$; $^{***}P < 0.001$

sFRP5 was possibly due to its DNA hypermethylation in renal tubular cells after IS treatment. It has been shown that *sFRP5* is the specific antagonist of Wnt5a [39, 40]. Our further investigation demonstrated that IS significantly inhibited the binding of *sFRP5* to Wnt5a, which might have contributed to the increased β-catenin expression. On the other hand, treatment with 5-Aza-2dc, an inhibitor of DNMTs, substantially reduced the IS-induced DNA hypermethylation and downregulation of *sFRP5* in renal tubular cells. Moreover, intraperitoneal injections of both 5-Aza-2dc and recombinant *sFRP5* protein significantly alleviated the IS-induced activation of Wnt/β-catenin and renal fibrosis. A previous study has shown that klotho DNA hypermethylation induced by indoxyl sulfate also caused renal fibrosis through downregulation of the expression of klotho [23]. Additionally, Zhou et al. reported that klotho is an endogenous Wnt antagonist; loss of klotho promotes kidney injury by derepression of Wnt/β-catenin signaling [29]. In the present study, we also observe the decreased expression of klotho in kidneys of IS-injected mice and IS-treated HK-2 cells, and further confirm that IS could activate Wnt/β-catenin signaling and promote renal fibrosis through the induction of *sFRP5* DNA hypermethylation. Therefore,

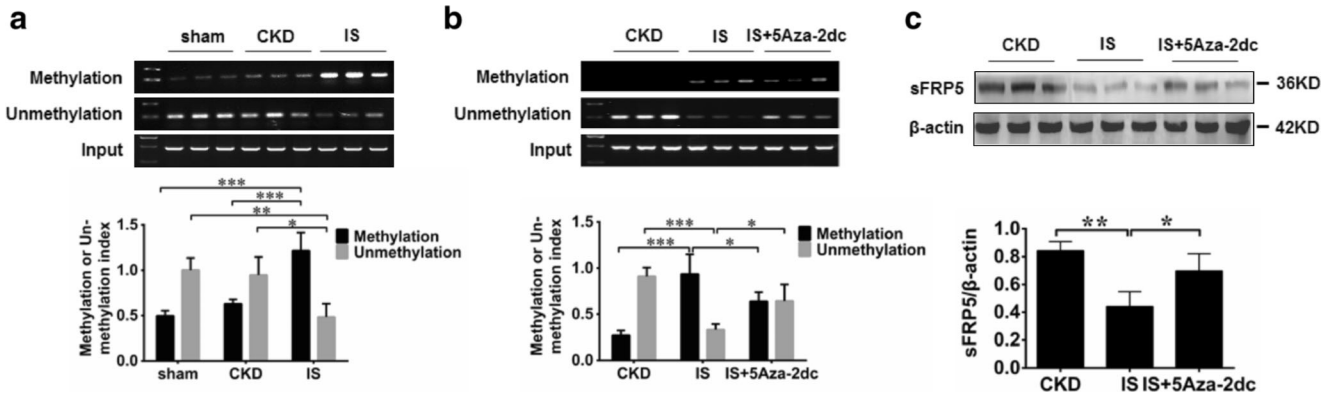

Fig. 7 5-Aza-2dc inhibits the DNA hypermethylation of *sFRP5* in IS-injected CKD mice. **a**, **b** In uninephrectomized mice, intraperitoneal injections of 0.01 mg/kg/day IS increased the *sFRP5* DNA methylation level in the kidney, but simultaneous injections of 0.35 mg/kg/48 h 5-Aza-2dc alleviated the effect of IS, as determined by the MSP results. **c** The DNA methylation inhibitor 5-Aza-2dc reversed the decrease in *sFRP5* protein expression in the kidney in IS-injected CKD mice. Data are the means ± SEM. $^{**}P < 0.01$; $^{***}P < 0.001$ ($n = 8$ mice)

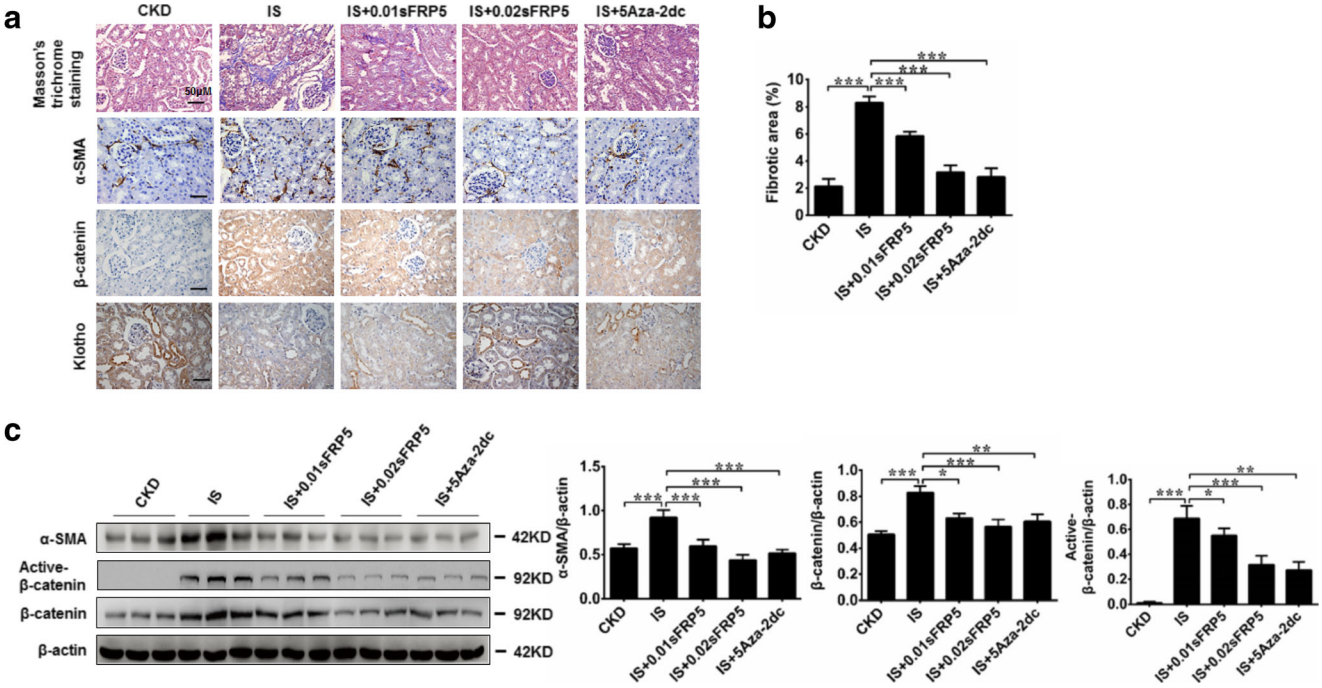

Fig. 8 Recombinant *sFRP5* protein and 5-Aza-2dc treatments ameliorate renal fibrosis through inhibiting Wnt/β-catenin signaling in IS-injected CKD mice. **a** Representative Masson's trichrome staining, Sirius red staining, and immunohistochemical staining of β-catenin, α-SMA, and klotho in the kidney. **b** Quantification of fibrotic area (*blue area*). **c**, **d** The protein expression of β-catenin, active-β-catenin, and α-SMA in the kidney, as revealed by western blotting. Data are the means ± SEM.*$P < 0.05$; **$P < 0.01$; ***$P < 0.001$ ($n = 8$ mice)

we deduce that both klotho and *sFRP5* DNA hypermethylation play a key role in IS-induced the activation of Wnt signaling and renal fibrosis.

Previous studies have shown that oxidative stress is a major cause of the aberrant DNA methylation of target genes [41–43], and serum IS levels have been shown to be associated with increased oxidative stress in CKD patients [44]. Therefore, we further investigated the mechanism underlying the effect of IS on *sFRP5* DNA hypermethylation and found that the IS-induced hypermethylation of *sFRP5* was inhibited by a ROS scavenger and an ERK1/2 inhibitor, indicating that oxidative stress-mediated ERK1/2 signaling is involved in the IS-induced DNA hypermethylation of *sFRP5*. These findings also provide a deeper understanding of the pathological role of oxidative stress in the progression of renal fibrosis.

In conclusion, we not only addressed the role of protein-bound uremic toxins accumulation in inducing renal fibrosis but also revealed that IS-induced *sFRP5* DNA hypermethylation is an important contributor to the activation of the Wnt/β-catenin signaling that plays a key role in renal fibrosis, thereby providing novel insight into the mechanisms underlying the effect of protein-bound uremic toxins on the progression of renal fibrosis in CKD. As the progression of renal fibrosis may aggravate the renal dysfunction, which in turn promotes uremic toxins accumulation, our findings also provide a deeper understanding of the progressive renal lesion in CKD.

Materials and methods

Selection of patients

Thirty-four patients (aged 22–78 years) with primary chronic renal diseases were recruited from the Department of Nephrology of Xinqiao Hospital (Chongqing, China). The following exclusion criteria were applied: polycystic kidney disease, pregnancy, human immunodeficiency virus, renal cancer, and recent immunosuppressive therapy. Kidney biopsies and serum samples were obtained from these patients for subsequent Masson's trichrome staining and IS measurements. The study protocol was approved by the Ethics Committee of Xinqiao Hospital and carried out in accordance with the Declaration of Helsinki.

Mice

Six-week-old male CD-1 mice were purchased from Beijing Vital River Laboratory Animal Technology Co., Ltd. (Beijing, China) and randomized into different groups: (1) sham group (mice underwent kidney-exposure operations only), (2) CKD group (½ nephrectomy: right kidney was removed and intraperitoneal injections of 0.01 mol/L PBS were administered), (3) IS group (CKD+IS, mean that CKD mice injected with 100 mg/kg/day IS (Sigma-Aldrich, USA)), (4) IS+5-Aza-2dc group (CKD+IS+5-Aza-2dc, mean that IS-injected CKD mice

received simultaneous intraperitoneal injections of 0.35 mg/kg/48 h 5-Aza-2dc (Sigma-Aldrich, USA) for 4 weeks), (5) IS+0.01 *sFRP5* group (CKD+IS+*sFRP5* at 0.01 mg/kg/48 h, mean that IS-injected CKD mice received recombinant mouse *sFRP5* protein (R&D Systems, Minneapolis, USA) at a dosage of 0.01 mg/kg/48 h for 4 weeks), and (6) IS+0.02 *sFRP5* group (CKD+IS+*sFRP5* at 0.02 mg/kg/48 h for 4 weeks). Mice were euthanized after injection for 4 weeks, and kidney and blood samples were collected for further analysis. All animal studies were approved by the Institutional Animal Care and Use Committee of Third Military Medical University and were carried out in accordance with the institutional animal care guidelines established by the Third Military Medical University.

IS measurement

The IS serum levels of mice were detected by high-performance liquid chromatography (HPLC) as described previously [25].

Masson's trichrome staining

The paraffin sections of the kidneys were stained with Masson's trichrome, and the quantification of the fibrotic area was carried out using Image Pro-Plus 6.0 software (Bethesda, MD) as described previously [25].

Sirius red staining

The paraffin sections of the kidneys were stained with Sirius red staining and picro-sirius red for light microscope examination which was described before [45, 46]. Briefly, kidney tissues were embedded in paraffin after being fixed in 10% formalin for 24 h. Three-micrometer paraffin sections were mounted on glass slides, then stained for 30 min with Sirius red (0.1% of Sirius red in saturated aqueous picric acid) [45]. Sections were then observed under polarized light microscopy (Olympus BX63, Tokyo, Japan). Under polarized light, the larger collagen fibers (type I) are bright yellow or orange [46].

Immunohistochemistry

Kidney tissues were embedded in paraffin after being fixed in 10% formalin for 24 h. Immunohistochemical staining was performed using standard methods. The following primary antibodies were used: rabbit polyclonal anti-*sFRP5* (Abcam, Cambridge, UK), rabbit polyclonal anti-β-catenin (Cell Signaling Technology, Beverly, MA, USA), rabbit monoclonal anti-klotho (Abcam, Cambridge, UK) and rabbit monoclonal anti-α-SMA (Millipore, Merck KGaA, Germany). After incubation with primary antibodies at 4 °C overnight, the slides were then incubated with enzyme-conjugated secondary antibodies and developed with 3,3′-diaminobenzidine (DAB). Slides were observed with an inverted microscope (Olympus BX63, Tokyo, Japan). The negative controls were performed using PBS to replace the primary antibody. Images were gathered from randomly selected microscopic fields.

Cell culture

The human renal proximal tubule epithelial cells (HK-2) were purchased from the American Type Culture Collection (ATCC; Manassas, VA, USA), and the cells were cultured in a DMEM/high glucose medium supplemented with 10% fetal bovine serum (Gibco Invitrogen, Carlsbad, CA, USA) and 1% penicillin/streptomycin at 37 °C in a 5% CO_2 humidified incubator.

Methylation-specific PCR and BSP

Genomic DNA was extracted using a Quick-gDNA MiniPrep kit (Zymo Research, Irvine, CA) and modified with a bisulfate treatment according to the manufacturer's instructions for the EZ DNA Methylation Gold Kit (Zymo Research, Irvine, CA). The gene promoter-specific primers that recognize the methylated and unmethylated CpG sites for the *sFRP5* and BSP primers were designed by MethPrimer software (http://www.urogene.org/cgi-bin/methprimer/methprimer.cgi) and listed in Supplement Table S1. The PCR products of genomic DNA without bisulfate treatment were used as control for the MSP. The T100™ PCR amplification system (Bio-Rad, Hercules, CA) was used for the MSP and BSP extensions. PCR products for MSP were visualized by gold-view staining in 3% agarose gels, and the densitometric intensity corresponding to each band was quantified by Quantity One software (Bio-Rad). Each reaction was performed in triplicate. For the quantitative methylation analysis, BSP was carried out by subcloning the PCR products into pGEM-T Easy Vectors (Promega, Madison, USA), which were then transformed into *Escherichia coli* DH5α. More than ten candidate plasmid clones were selected for sequencing (Beijing Genome Institute, Beijing, China).

RT-PCR

Total RNA of cells and tissues was extracted with RNAiso Plus according to the manufacturer's protocol, and samples were quantified using a NanoDrop spectrophotometer. Reverse transcription was carried out using a Reverse Transcription Kit (TaKaRa Bio; Otsu, Shiga Prefecture, Japan). The PCR reaction was performed in a programmable thermal cycler. The primers used in the experiments are presented in supplementary Table S2.

Western blotting

The protein samples isolated from HK-2 cells and kidney tissue were used to perform western blotting as described previously [47]. The following primary antibodies were used: rabbit monoclonal anti-α-SMA (42 kD, 1:1000, Millipore, Merck KGaA, Germany), rabbit monoclonal anti-β-catenin (92 kD, 1:3000, Abcam, Cambridge, UK), rabbit monoclonal anti-active-β-catenin (92 kD, 1:1000, Millipore, Merck KGaA, Germany), rabbit monoclonal anti-klotho (116 kD, 1:1000, Abcam, Cambridge, UK), rabbit polyclonal anti-*sFRP5* (36 kD, 1:1000, Abcam, Cambridge, UK), rabbit monoclonal anti-phospho-ERK1/2, rabbit polyclonal anti-ERK1/2 (42, 44 kD, 1:1000, Cell Signaling Technology, Beverly, MA, USA), rabbit monoclonal anti-DNMT1 (200 kD, 1:1000, Cell Signaling Technology, Beverly, MA, USA), rabbit polyclonal anti-DNMT3a (100–130 kD, 1:1000, Santa Cruz Biotechnology, Santa Cruz, CA), rabbit polyclonal anti-DNMT3b (75–100 kD, 1:1000, Santa Cruz Biotechnology, Santa Cruz, CA), and mouse monoclonal anti-β-actin (42 kD, Santa Cruz Biotechnology, Dallas, TX, USA).

Immunoprecipitation

HK-2 cells were incubated with 50 mg/L IS in the presence or absence of 10 μmol/L 5-Aza-2dc for 72 h at 37 °C. Immunoprecipitation was performed using a Pierce Classic IP kit (Thermo Scientific, Rockford, IL, USA) according to the manufacturer's instructions. Briefly, cell lysates were incubated with 4 μL of rabbit polyclonal anti-Wnt5a (Millipore, Merck KGaA, Germany) or 4 μL of rabbit anti-IgG (Santa Cruz Biotechnology, Santa Cruz, CA) at 4 °C overnight. Then, the precipitated complexes were captured by 20 μL of Protein A/G agarose, followed by western blotting with rabbit polyclonal anti-*sFRP5* and rabbit polyclonal Wnt5a, respectively.

ROS measurement

Intracellular ROS levels were measured using the dichlorodihydrofluorescein diacetate (DCFH-DA) assay. The cells were incubated in 96-well plates for 24 h and then incubated with 50 mg/L IS for different times (15, 30, 60, and 180 min), or they were incubated with different concentrations of IS (2, 10, and 50 mg/L) for 3 h. Subsequently, cells were loaded in the dark for 30 min with DMEM containing 10 μmol/L DCFH-DA at 37 °C. After washing twice with sterile PBS, the cells were observed under a fluorescence microscope (Olympus IMT-2, Tokyo, Japan). To quantify ROS production, the relative intensity of DCF fluorescence was detected using a fluorometric imaging plate reader (Thermo Fisher Scientific, Pittsburgh, PA, USA) at excitation and emission wavelengths of 488 and 520 nm, respectively.

Statistical analysis

BSP sequence data were analyzed using software from BiQ Analyzer. The data from other experiments are presented as the means ± SEM. Statistical analyses were performed using SPSS 19.0 (SPSS Japan, Tokyo, Japan) and GraphPad Prism 6 (GraphPad Software Inc., San Diego, CA). Tukey's post hoc analyses were used to determine significant differences among three or more groups. The criteria for significance were defined as $p < 0.05$.

Acknowledgments This study was supported by research grants from the National Natural Science Foundation of China (Nos. 81500567, 81500544, 81270290, and 81400747) and the project for Chongqing basic science and advanced technology research (cstc2015jcyjBX0028).

Compliance with ethical standards The study protocol was approved by the Ethics Committee of Xinqiao Hospital and carried out in accordance with the Declaration of Helsinki.

Conflict of interest The authors declare that they have no conflict of interest.

References

1. Nangaku M (2006) Chronic hypoxia and tubulointerstitial injury: a final common pathway to end-stage renal failure. J Am SocNephrol 17(1):17–25
2. Zeisberg M, Neilson EG (2010) Mechanisms of tubulointerstitial fibrosis. J Am SocNephrol 21(11):1819–1834
3. Nath KA (1992) Tubulointerstitial changes as a major determinant in the progression of renal damage. Am J Kidney Dis 20(1):1–17
4. Ruiz-Ortega M, Egido J (1997) Angiotensin II modulates cell growth-related events and synthesis of matrix proteins in renal interstitial fibroblasts. Kidney Int 52(6):1497–1510
5. Chade AR, Mushin OP, Zhu X, Rodriguez-Porcel M, Grande JP, Textor SC, Lerman A, Lerman LO (2005) Pathways of renal fibrosis and modulation of matrix turnover in experimental hypercholesterolemia. Hypertension 46(4):772–779
6. Lin CL, Wang JY, Ko JY, Huang YT, Kuo YH, Wang FS (2010) Dickkopf-1 promotes hyperglycemia-induced accumulation of mesangial matrix and renal dysfunction. J Am SocNephrol 21(1): 124–135
7. Kim J, Seok YM, Jung KJ, Park KM (2009) Reactive oxygen species/oxidative stress contributes to progression of kidney fibrosis following transient ischemic injury in mice. Am J Physiol Renal Physiol 297(2):F461–F470
8. Duranton F, Cohen G, De Smet R, Rodriguez M, Jankowski J, Vanholder R, Argiles A, European Uremic Toxin Work Group (2012) Normal and pathologic concentrations of uremic toxins. J Am SocNephrol 23:1258–1270
9. Wu IW, Hsu KH, Hsu HJ, Lee CC, Sun CY, Tsai CJ, Wu MS (2012) Serum free p-cresyl sulfate levels predict cardiovascular and all-cause mortality in elderly hemodialysis patients-a prospective cohort study. Nephrol Dial Transplant 27:1169–1175

10. Barreto FC, Barreto DV, Liabeuf S, Meert N, Glorieux G, Temmar M, Choukroun G, VanholderR MZA, European Uremic Toxin Work Group (EUTox) (2009) Serum indoxyl sulfate is associated with vascular disease and mortality in chronic kidney disease patients. Clin J Am SocNephrol 4(10):1551–1558
11. Lekawanvijit S, Adrahtas A, Kelly DJ, Kompa AR, Wang BH, Krum H (2010) Does indoxyl sulfate, a uraemic toxin, have direct effects on cardiacfibroblasts and myocytes? Eur Heart J 31(14): 1771–1779
12. Lin CJ, Pan CF, Liu HL, Chuang CK, Jayakumar T, Wang TJ, Chen HH, Wu CJ (2012) The role of protein-bound uremic toxins on peripheral artery disease and vascular access failure in patients on hemodialysis. Atherosclerosis 225(1):173–179
13. Watanabe H, Miyamoto Y, Honda D, Tanaka H, Wu Q, Endo M, Noguchi T, Kadowaki D, Ishima Y, Kotani S et al (2013) p-Cresyl sulfate causes renaltubular cell damage by inducing oxidative stress by activation of NADPH oxidase. Kidney Int 83(4):582–592
14. Sun CY, Hsu HH, Wu MS (2013) p-Cresol sulfate and indoxylsulfate induce similar cellular inflammatory gene expressions in cultured proximal renaltubular cells. Nephrol Dial Transplant 28(1):70–78
15. Shimizu H, Bolati D, Adijiang A, Muteliefu G, Enomoto A, Nishijima F, Dateki M, Niwa T (2011) NF-κB plays an important role in indoxylsulfate-induced cellular senescence, fibrotic gene expression, and inhibition of proliferation in proximal tubular cells. Am J Physiol Cell Physiol 301(5):C1201–C1212
16. He W, Dai C, Li Y, Zeng G, Monga SP, Liu Y (2009) Wnt/beta-catenin signaling promotes renal interstitial fibrosis. J Am SocNephrol 20(4):765–776
17. Surendran K, Schiavi S, Hruska KA (2005) Wnt-dependent beta-catenin signaling is activated after unilateral ureteral obstruction, and recombinant secreted frizzled-related protein 4 alters the progression of renal fibrosis. J Am SocNephrol 16(8):2373–2384
18. Finch PW, He X, Kelley MJ, Uren A, Schaudies RP, Popescu NC, Rudikoff S, Aaronson SA, Varmus HE, Rubin JS (1997) Purification and molecular cloning of a secreted, frizzled-related antagonist of Wnt action. Proc Natl Acad Sci U S A 94(13): 6770–6775
19. Xie Q, Chen L, Shan X, Shan X, Tang J, Zhou F, Chen Q, Quan H, Nie D, Zhang W et al (2014) Epigenetic silencing of SFRP1 and SFRP5 by hepatitis B virus X protein enhances hepatoma cell tumorigenicity through Wnt signalling pathway. Int J Cancer 135: 635–646
20. Saito T, Mitomi H, Imamhasan A, Hayashi T, Mitani K, Takahashi M, Kajiyama Y, Yao T (2014) Downregulation of sFRP-2 by epigenetic silencing activates the β-catenin/Wnt signaling pathway in esophageal basaloid squamous cell carcinoma. Virchows Arch 464(2):135–143
21. Stenvinkel P, Karimi M, Johansson S, Axelsson J, Suliman M, Lindholm B, Heimbürger O, Barany P, Alvestrand A, Nordfors L et al (2007) Impact of inflammationon epigenetic DNA methylation–a novel risk factor for cardiovascular disease? J Intern Med 261(1):488–499
22. Hori Y, Oda Y, Kiyoshima K, Yamada Y, Nakashima Y, Naito S, Tsuneyoshi M (2007) Oxidative stress and DNA hypermethylation status in renal cell carcinoma arising in patients on dialysis. J Pathol 212(2):218–226
23. Sun CY, Chang SC, Wu MS (2012) Suppression of Klotho expression by protein-bound uremic toxins is associated with increased DNA methyltransferase expression and DNA hypermethylation. Kidney Int 81(7):640–650
24. Vanholder R, Schepers E, Pletinck A, Nagler EV, Glorieux G (2014) The uremic toxicity of indoxyl sulfate and p-cresyl sulfate: a systematic review. J Am SocNephrol 25(9):1897–1907
25. Yang K, Wang C, Nie L, Zhao X, Gu J, Guan X, Wang S, Xiao T, Xu X, He T et al (2015) Klotho protects against IS-induced myocardial hypertrophy. J Am Soc Nephrol 26(10):2434–2446
26. Grigoryan T, Wend P, Klaus A, Birchmeier W (2008) Deciphering the function of canonical Wnt signals indevelopment and disease: conditional loss- and gain-of-function mutations of beta-catenin in mice. Genes Dev 22(17):2308–2341
27. He W, Tan RJ, Li Y, Wang D, Nie J, Hou FF, Liu Y (2012) Matrix metalloproteinase-7 as a surrogate marker predicts renal Wnt/beta-catenin activity in CKD. J Am Soc Nephrol 23(2):294–304
28. Nelson PJ, von Toerne C, Gröne HJ (2011) Wnt-signaling pathways in progressive renal fibrosis. Expert OpinTher Targets 15(9):1073–1083
29. Zhou L, Li Y, Zhou D, Tan RJ, Liu Y (2013) Loss of Klotho contributes to kidney injury by derepression of Wnt/β-catenin signaling. J Am Soc Nephrol 24(5):771–785
30. Zhou L, Li Y, Hao S, Zhou D, Tan RJ, Nie J, Hou FF, Kahn M, Liu Y (2015) Multiple genes of the renin-angiotensin system are novel targets of Wnt/β-catenin signaling. J Am Soc Nephrol 26(1):107–120
31. Boutet A, De Frutos CA, Maxwell PH, Mayol MJ, Romero J, Nieto MA (2006) Snail activation disrupts tissue homeostasis and induces fibrosis in the adult kidney. EMBO J 25(23):5603–5613
32. Bafico A, Gazit A, Pramila T, Finch PW, Yaniv A, Aaronson SA (1999) Interaction of frizzled related protein (FRP) with Wnt ligands and the frizzled receptor suggests alternative mechanisms for FRP inhibition of Wnt signaling. J Biol Chem 274(23): 16180–16187
33. Surana R, Sikka S, Cai W, Shin EM, Warrier SR, Tan HJ, Arfuso F, Fox SA, Dharmarajan AM, Kumar AP (2014) Secreted frizzled related proteins: implications in cancers. Biochim Biophys Acta 1845(1):53–65
34. Shulewitz M, Soloviev I, Wu T, Koeppen H, Polakis P, Sakanaka C (2006) Repressor roles for TCF-4 and Sfrp1 in Wnt signaling in breast cancer. Oncogene 25(31):4361–4369
35. Horvath LG, Henshall SM, Kench JG, Saunders DN, Lee CS, Golovsky D, Brenner PC, O'Neill GF, Kooner R, Stricker PD et al (2004) Membranous expression of secreted frizzled-related protein 4 predicts for good prognosis in localized prostate cancer and inhibits PC3 cellular proliferation in vitro. Clin Cancer Res 10(2):615–625
36. Matsuyama M, Nomori A, Nakakuni K, Shimono A, Fukushima M (2014) Secreted Frizzled-related protein 1 (Sfrp1) regulates the progression of renal fibrosis in a mouse model of obstructive nephropathy. J Biol Chem 289(45):31526–31533
37. Kaur P, Mani S, Cros MP, Scoazec JY, Chemin I, Hainaut P, Herceg Z (2012) Epigenetic silencing of sFRP1 activates the canonical Wnt pathway and contributes to increased cell growth and proliferation in hepatocellular carcinoma. Tumour Biol 33(2):325–336
38. Perry AS, O'Hurley G, Raheem OA, Brennan K, Wong S, O'Grady A, Kennedy AM, Marignol L, Murphy TM, Sullivan L et al (2013) Gene expression and epigenetic discovery screen reveal methylation of SFRP2 in prostate cancer. Int J Cancer 132(8):1771–1780
39. Ouchi N, Higuchi A, Ohashi K, Oshima Y, Gokce N, Shibata R, Akasaki Y, Shimono A, Walsh K (2010) Sfrp5 is an anti-inflammatory adipokine that modulates metabolic dysfunction in obesity. Science 329:454–457
40. Zhao C, Bu X, Wang W, Ma T, Ma H (2014) GEC-derived SFRP5 inhibits Wnt5a-induced macrophage chemotaxis and activation. PLoS One 9(1):e85058
41. Stenvinkel P, Carrero JJ, Axelsson J, Lindholm B, Heimbürger O, Massy Z (2008) Emerging biomarkers for evaluating cardiovascular risk in the chronic kidney disease patient: how do new pieces fit into the uremic puzzle? Clin J Am SocNephrol 3(2):505–521
42. Ingrosso D, Cimmino A, Perna AF, Masella L, De Santo NG, De Bonis ML, Vacca M, D'Esposito M, D'Urso M, Galletti P et al

(2003) Folate treatment and unbalanced methylation and changes of allelic expression induced by hyperhomocysteinaemia in patients with uraemia. Lancet 361(9370):1693–1699

43. Jiang Y, Sun T, Xiong J, Cao J, Li G, Wang S (2007) Hyperhomocysteinemia-mediated DNA hypomethylation and its potential epigenetic role in rats. Acta Biochim Biophys Sin Shanghai 39(9):657–667
44. Rossi M, Campbell KL, Johnson DW, Stanton T, Vesey DA, Coombes JS, Weston KS, Hawley CM, McWhinney BC, Ungerer JP et al (2014) Protein-bound uremic toxins, inflammation and oxidative stress: a cross-sectional study in stage 3-4 chronic kidney disease. Arch Med Res 45(4):309–317
45. Lattouf R, Younes R, Lutomski D, Naaman N, Godeau G, Senni K, Changotade S (2014) Picrosirius red staining: a useful tool to appraise collagen networks in normal and pathological tissues. J Histochem Cytochem 62(10):751–758
46. Zhao YY, Chen H, Tian T, Chen DQ, Bai X, Wei F (2014) A pharmaco-metabonomic study on chronic kidney disease and therapeutic effect of ergone by UPLC-QTOF/HDMS. PLoS One 9(12): e115467
47. Guan X, Nie L, He T, Yang K, Xiao T, Wang S, Huang Y, Zhang J, Wang J, Sharma K (2014) Klotho suppresses renal tubulointerstitial fibrosis by controlling basic fibroblast growth factor-2 signalling. J Pathol 234(4):560–572